

See discussions, stats, and author profiles for this publication at: <https://www.researchgate.net/publication/50935210>

Chang, Y., Shih, Y. J., Ko, C. Y., Jhong, J. F., Liu, Y. L. & Wei, T. C. Hemocompatibility of poly(vinylidene fluoride) membrane grafted with network-like and brush-like antifoulin...

ARTICLE *in* LANGMUIR · MARCH 2011

Impact Factor: 4.46 · DOI: 10.1021/la1048369 · Source: PubMed

CITATIONS

59

READS

108

6 AUTHORS, INCLUDING:



[Yung Chang](#)

Chung Yuan Christian University

138 PUBLICATIONS 2,942 CITATIONS

[SEE PROFILE](#)



[Ying-Ling Liu](#)

National Tsing Hua University

185 PUBLICATIONS 5,886 CITATIONS

[SEE PROFILE](#)

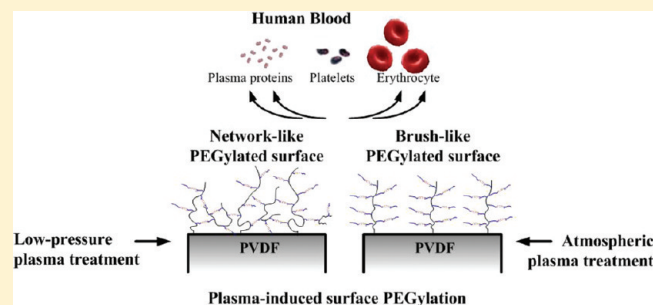
Hemocompatibility of Poly(vinylidene fluoride) Membrane Grafted with Network-Like and Brush-Like Antifouling Layer Controlled via Plasma-Induced Surface PEGylation

Yung Chang,* Yu-Ju Shih, Chao-Yin Ko, Jheng-Fong Jhong, Ying-Ling Liu, and Ta-Chin Wei*

R&D Center for Membrane Technology and Department of Chemical Engineering, Chung Yuan Christian University, Chung-Li, Taoyuan 320, Taiwan

ABSTRACT: In this work, the hemocompatibility of PEGylated poly(vinylidene fluoride) (PVDF) microporous membranes with varying grafting coverage and structures via plasma-induced surface PEGylation was studied. Network-like and brush-like PEGylated layers on PVDF membrane surfaces were achieved by low-pressure and atmospheric plasma treatment. The chemical composition, physical morphology, grafting structure, surface hydrophilicity, and hydration capability of prepared membranes were determined to illustrate the correlations between grafting qualities and hemocompatibility of PEGylated PVDF membranes in contact with human blood.

Plasma protein adsorption onto different PEGylated PVDF membranes from single-protein solutions and the complex medium of 100% human plasma were measured by enzyme-linked immunosorbent assay (ELISA) with monoclonal antibodies. Hemocompatibility of the PEGylated membranes was evaluated by the antifouling property of platelet adhesion observed by scanning electron microscopy (SEM) and the anticoagulant activity of the blood coagulant determined by testing plasma-clotting time. The control of grafting structures of PEGylated layers highly regulates the PVDF membrane to resist the adsorption of plasma proteins, the adhesion of platelets, and the coagulation of human plasma. It was found that PVDF membranes grafted with brush-like PEGylated layers presented higher hydration capability with binding water molecules than with network-like PEGylated layers to improve the hemocompatible character of plasma protein and blood platelet resistance in human blood. This work suggests that the hemocompatible nature of grafted PEGylated polymers by controlling grafting structures gives them great potential in the molecular design of antithrombogenic membranes for use in human blood.



INTRODUCTION

Hemocompatibility is highly desirable for important biomedical applications with blood-contacting devices used in hemodialysis membranes, antithrombogenic implants, and biomedical sensors.^{1–5} However, only a few synthesized polymeric membranes are regarded as good blood-contacting systems. In general, polymeric membranes prepared from hydrophobic materials in contact with blood will lead to the adsorption of plasma protein such as fibrinogen and the clotting enzymes on those membrane surfaces.^{6,7} Then, introduced full-scale blood platelet adhesion results in the formation of thrombosis and embolism at the blood contact side of membrane surfaces from the bloodstream. It is believed that the increase of hydrophilic moieties on a hydrophobic material surface can effectively reduce blood–material interactions inducing thrombogenic response between the blood cells and the hydrophobic surface.^{4–6} Surface modification is considered a promising approach to incorporate blood inert functionalities onto a wide range of hydrophobic membrane materials for improved hemocompatibility.^{8–10} Therefore, an ideal hemocompatible membrane can be designed with a combination of the excellent mechanical bulk properties of hydrophobic materials and the good antithrombogenic surface characteristics of strong hydrophilic polymer layers.^{10–13}

Fluoro-based membranes such as poly(vinylidene fluoride) (PVDF) exhibit a wide range of outstanding properties, including high-temperature stability, excellent chemical resistance, and low water sorption.^{14,15} For the improved antifouling properties of PVDF membranes, they have been widely studied via surface modification to introduce hydrophilic groups in order to alter their membrane surface properties.^{9,12,13,16–23} One of the most important requirements for PVDF as a blood-contacting membrane is to reduce the nonspecific adsorption of plasma proteins when their hydrophobic surfaces are encountered in the bloodstream.⁹ Hydrophilic materials such as poly(ethylene glycol) (PEG)-based material have been shown to effectively resist nonspecific protein adsorption. Several strategies have been adopted to graft PEG-based polymer layers from hydrophobic PVDF surfaces through surface pretreatment, such as activation by electron beam, gas plasma, ozone, or UV treatment, and followed by surface-initiated polymerization.^{9,12,16–24} We have performed grafting of hemocompatible PVDF membranes

Received: December 5, 2010

Revised: February 13, 2011

Published: March 30, 2011

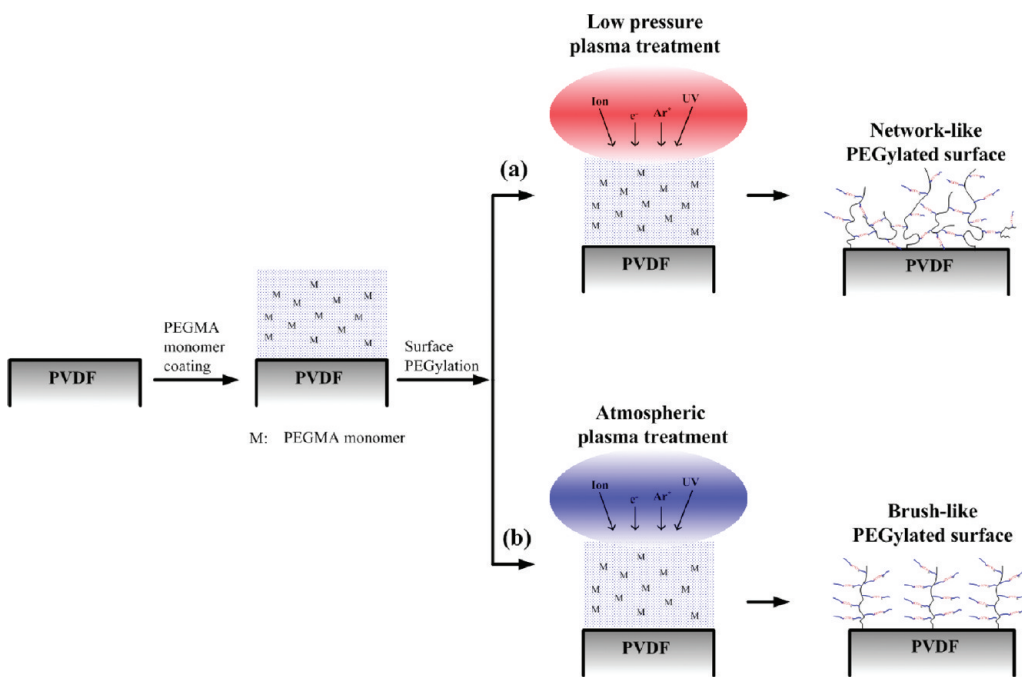


Figure 1. Schematic illustration of the preparation process of the PVDF-g-PEGMA membranes via plasma-induced surface PEGylation: (a) low-pressure plasma treatment; (b) atmospheric plasma treatment.

with PEGylated layers using a multistep surface modification procedure from a combination of ozone-pretreatment and thermal-induced copolymerization.⁹ However, typical approaches lack efficient grafting control to process the surface PEGylation on PVDF membranes due to their excellent chemical resistance and strong hydrophobicity. In this work, a new approach of the atmospheric plasma technique was first developed to control the surface PEGylation and hemocompatibility of PEGylated layers on PVDF membranes.

Previous studies show that the control of surface grafting coverage is important for a PEGylated membrane with an antifouling surface. It was reported that the PEGylated PVDF membrane provides good resistance to protein adsorption, while surface grafting of PEGylated layer is fully covered.^{9,12,16–24} Although the plasma protein resistance of PEGylated PVDF membrane surfaces with varying grafting coverage has been studied,⁹ it is still unclear how grafting structures of PEGylated layers would influence the correlation between surface PEGylation and hemocompatibility. It is also important to understand the effects of both grafting coverage and structures of PEGylated layers on the hydration properties of PEG chains, and the results from such studies would directly enable the rational design of PEGylated membranes for use in blood-contacting applications. In the present work, we developed new surface grafting control of PVDF membranes with poly(ethylene glycol) methacrylate (PEGMA) via plasma-induced interfacial copolymerization, which was carried out by low-pressure and atmospheric plasma treatments. Two different surface grafting structures of a PEGylated layer, network-like PEGMA, and brush-like PEGMA, on a PVDF membrane surface were achieved in this study. The effects of different plasma treatments on the grafting structures of these PEGylated membranes with various grafting coverage were examined in detail. The adsorption of plasma proteins and the adhesion of platelets onto the PEGylated membrane surface from human blood plasma was also demonstrated along with the

anticoagulant activity of the membranes in recalcified plasma-clotting tests from a platelet-poor plasma solution. This study not only introduces new surface grafting control of atmospheric plasma-induced PEGylation on chemically inert PVDF membranes but also provides a fundamental understanding of various PEGylated grafting coverage and structures governing the performance of antifouling properties associated with their hemocompatibility.

MATERIALS AND METHODS

Materials. PVDF microporous membranes with an average pore size of 0.1 μm , a thickness of about 110 μm , and a diameter of 47 mm were purchased from the Millipore Co. (VVHP04700) and were used as received. Poly(ethylene glycol) methacrylate (PEGMA) macromonomers with a molecular weight of about 500 Da and an average number of ethylene glycol units of about 10 were purchased from Aldrich. Isopropanol (IPA) was obtained from Aldrich and was used as a solvent for the plasma-induced graft polymerization. Fibrinogen (fraction I from human plasma) was purchased from Sigma Chemical Co. Human blood and plasma solution was obtained from Taiwan Blood Services Foundation. Phosphate buffered saline (PBS) was purchased from Sigma-Aldrich. Deionized water used in experiments was purified using a Millipore water purification system with a minimum resistivity of 18.0 M Ω m.

Surface PEGylation. A schematic illustration of the plasma-induced surface PEGylation on PVDF membranes under the control of low-pressure or atmospheric plasma treatment is shown in Figure 1. The PVDF membrane of about 0.4 cm^2 in surface area was first incubated in an IPA solution containing 10 wt % of PEGMA monomer. After the drying process of the PEGMA-coated PVDF membrane at 25 °C for 24 h, the membrane coated with a dried PEGMA monomer layer of ~1.0 mg/cm² was then treated by low-pressure plasma or atmospheric plasma with argon flow rate of 10 slm and input power of 150 W controlled by a 13.56 MHz RF generator (Cesar 136, Dressler). The low-pressure plasma treatment was operated at 0.5 Torr. After

plasma treatment, the PEGylated PVDF membrane was transferred into purified methanol and was then extracted with deionized water and methanol, respectively, each for 60 min in the ultrasonic device to strip off PEGMA homopolymers and unreacted monomers. The residual solvent was removed in a vacuum oven under reduced pressure for 3 days. In this study, all membranes after plasma treatment were cleaned under the same postwash procedures.

Surface Characterization. The chemical composition of surface-modified PVDF membranes with grafted PEGMA layer was characterized using FT-IR spectrophotometry (Perkin-Elmer Spectrum One) with ZnSe as an internal reflection element. Each spectrum was captured by averaging 32 scans at a resolution of 4 cm^{-1} . The surface grafting yield of PEGMA on the PVDF membrane was determined by the extent of weight increase compared to the virgin PVDF membrane based on the unit surface area 1 cm^2 of PVDF membrane. Prior to the weight measurements, the membranes were dried overnight in a vacuum oven at 50°C for 3 days. The surface grafting structures of the PEGylated membranes were characterized by X-ray photoelectron spectroscopy (XPS). XPS analysis was performed using a Thermal Scientific K-Alpha spectrometer equipped with a monochromated Al K X-ray source ($1\text{ }486.6\text{ eV}$ photons). The energy of emitted electrons was measured with a hemispherical energy analyzer at pass energies ranging from 50 to 150 eV. All data were collected at a photoelectron takeoff angle of 45° with respect to the sample surface. The binding energy (BE) scale is referenced by setting the peak maximum in the C 1s spectrum to 284.6 eV. The high-resolution C 1s spectrum was fitted using a Shirley background subtraction and a series of Gaussian peaks. Water contact angles were measured with an Goniometer (Automatic Contact Angle Meter, model FTA1000, First Ten Ångstroms Co, Ltd. USA) at 25°C . The DI water was dropped on the sample surface at 10 different sites. The surface morphology of virgin and surface-modified PVDF membranes was examined by bioatomic force microscopy (bio-AFM). All AFM images were acquired with a JPK Instruments AG multimode NanoWizard (Germany). The instrument is equipped with a NanoWizard scanner and operated in air and liquid. For tapping-mode AFM, a commercial Si cantilever (TESP tip) of about 320 kHz resonant frequency from JPK was used. The relative humidity was less than 40%.

Plasma Protein Adsorption on the PEGylated PVDF Membranes. In this study, platelet poor plasma (PPP) solution containing plasma proteins was tested on the PEGylated membrane surface. Blood was obtained from a healthy human volunteer. PPP was prepared by centrifugation of the blood at 3000 rpm for 10 min. The adsorption of human plasma solution of albumin, γ -globulin, and fibrinogen on the membranes was evaluated, respectively, using the enzyme-linked immunosorbent assay (ELISA) according to the standard protocol as described briefly below. First, the membranes of 0.4 cm^2 surface area were placed in individual wells of a 24-well tissue culture plate, and each well was equilibrated with $1000\text{ }\mu\text{L}$ of PBS for 60 min at 37°C . Then, the membranes were soaked in $500\text{ }\mu\text{L}$ of 100% platelet poor plasma (PPP) solution. After 180 min of incubation at 37°C , the films were rinsed five times with $500\text{ }\mu\text{L}$ of PBS and then incubated in bovine serum albumin (BSA, purchased from Aldrich) for 90 min at 37°C to block the areas unoccupied by protein. The membranes were rinsed with PBS five times more, transferred to a new plate, and incubated in a $500\text{ }\mu\text{L}$ PBS solution. The membranes were incubated with primary monoclonal antibody that reacted with the human plasma protein (i.e., HSA or Fg) for 90 min at 37°C and then blocked with 10 mg/mL BSA in PBS solution for 24 h at 37°C . The membranes were subsequently incubated with the secondary monoclonal antibody, horseradish peroxidase (HRP)-conjugated immunoglobulins for 60 min at 37°C . The primary antibody was not used, and only the secondary antibody (goat F(ab)₂ antihuman immunoglobulin peroxidase conjugate antibody) treatment was performed for the assay of the amount of human γ -globulin adsorbed on the membranes from PPP solution for 90 min at 37°C . The membranes were rinsed five

times with $500\text{ }\mu\text{L}$ of PBS and transferred into clean wells, followed by the addition of $500\text{ }\mu\text{L}$ of PBS containing 1 mg/mL chromogen of $3,3',5,5'$ -tetramethylbenzidine, 0.05 wt % Tween 20, and 0.03 wt % hydrogen peroxide. After incubation for 20 min at 37°C , the enzyme-induced color reaction was stopped by adding $500\text{ }\mu\text{L}$ of 1 mmol/mL H_2SO_4 to the solution in each well, and finally, the absorbance of light at 450 nm was determined by a microplate reader. Protein adsorption on the membranes was normalized with respect to that on the virgin PVDF membrane as a reference. These measurements were carried out 6 times for each membrane ($n = 6$).

Blood Platelet Adhesion on the PEGylated PVDF Membranes. The PVDF membranes of 0.4 cm^2 surface area were placed in individual wells of a 24-well tissue culture plate, and each well was equilibrated with $1000\text{ }\mu\text{L}$ of phosphate buffered solution (PBS) for 2 h at 25°C . Blood was obtained from a healthy human volunteer. Platelet rich plasma (PRP) containing about 1×10^5 cells/mL was prepared by centrifugation of the blood at 1200 rpm for 10 min. The platelet concentration was determined by microscopy (Nikon TS 100F). For the test of unactivated platelet adhesion on the membranes, $200\text{ }\mu\text{L}$ aliquots of the PRP were directly placed on the PVDF surface in each well of the tissue culture plate and incubated for 120 min at 37°C . For the test of activated platelet adhesion on the membranes, $200\text{ }\mu\text{L}$ of the PRP, first recalcified by the addition of calcium (1 M CaCl_2 , $5\text{ }\mu\text{L}$), was placed on the PVDF surface in each well of the tissue culture plate and incubated for 120 min at 37°C . After the PVDF membranes were rinsed twice with $1000\text{ }\mu\text{L}$ of PBS, they were immersed in 2.5% glutaraldehyde of PBS for 48 h at 4°C to fix the adhered platelets and adsorbed proteins, then rinsed 2 times with $1000\text{ }\mu\text{L}$ of PBS and gradient-dried with ethanol in 0% v/v PBS, 10% v/v PBS, 25% v/v PBS, 50% v/v PBS, 75% v/v PBS, 90% v/v PBS, and 100% v/v PBS for 20 min in each step and dried in air. Finally, the samples were sputter-coated with gold prior to observation under JEOL JSM-5410 SEM operating at 7 keV.

Plasma-Clotting Time of the PEGylated PVDF Membranes. The anticoagulant activity of the prepared membranes was evaluated by testing plasma-clotting time in human plasma. Prior to the test, the PEGylated PVDF membranes with 0.4 cm^2 were placed in the 24-well plate. Human normal plasma (platelet poor) was prepared from anticoagulated human blood from three donors by centrifugation (1200 rpm for 10 min at 25°C followed by 3000 rpm for 10 min at 25°C). Plasma was recalcified to 20 mM CaCl_2 by the addition of calcium from a 1 M stock solution and shaked for 30 s at 37°C . Then, 0.5 mL plasma was immediately added to each well in a 24-well plate (Falcon, nontissue culture treated polystyrene). The clotting time of the plasma was determined as the time where the onset of the absorbance transition occurred by reading the absorbance at 660 nm using the PowerWave microplate spectrophotometer with programmed temperature control at 37°C . Each clotting time is reported as the average value of repeated measurements of six samples ($n = 6$).

■ RESULTS AND DISCUSSION

Surface PEGylation and Characterization. A new integrated process of plasma-induced surface PEGylation was developed to modify the chemically inert PVDF membrane with a well-controlled PEGMA-grafted layer. As illustrated in Figure 1, the surface coverage of the PEGMA-grafted layer on PVDF (PVDF-g-PEGMA) membranes can be first regulated by the amount of uniformly coated PEGMA monomer and then followed by the control of plasma treatment time under low pressure or atmospheric pressure. On the basis of a general understanding of gas plasma treatment and surface-induced copolymerization, the possible mechanism of the surface grafting reaction could be divided into two reaction stages. In the initial stage, energetic

Table 1. Surface PEGylation of the PVDF Membranes

surface PEGylation	conditions of PEGylation				surface grafting yield (mg/cm^2)	surface contact angle ($^\circ$)
	PEGMA reaction amount	temperature ($^\circ\text{C}$)	grafting time			
PEGylation-1 ^a	1.0 mg/cm^2	<50	0–120 s	0.00–0.69	20–120	
PEGylation-2 ^b	1.0 mg/cm^2	<50	0–120 s	0.00–0.45	30–120	
PEGylation-3 ^c	30 mg/mL	80	0–48 h	0.00–0.12	60–120	

^a Membranes prepared by plasma-induced surface PEGylation using low-pressure plasma treatment. ^b Membranes prepared by plasma-induced surface PEGylation using atmospheric plasma treatment. ^c Membranes prepared by ozone pretreatment and thermal-induced graft-polymerization.⁹

species (Ar metastables and ions) and UV radiation from plasma treatment could generate initiator radicals both in PEGMA monomer and on PVDF membrane surface. The initiator radicals may undergo the following two types of addition reactions: (i) the copolymerization of initiator radicals on the PVDF membrane surface to PEGMA monomer, and (ii) the polymerization of initiator radicals in PEGMA monomer to PEGMA monomer. The first reaction will result in the immobilization of PEGMA polymers from the PVDF membrane surface. The second reaction will result in the formation of PEGMA homopolymer on the PVDF membrane surface. In the subsequent stage, continued surface plasma treatment induces the scission of chemical bonding in PEGMA polymer chains and the generation of free radicals in both PEGMA polymer brushes and PEGMA homopolymer. Then, the cross-linking reaction by recombination of free radicals might occur between PEGMA homopolymer chains and the PVDF membrane surface, PEGMA polymer brushes, or PEGMA homopolymer chains. Thus, the grafting structures of PEGylated layers on the PVDF-g-PEGMA membrane surface might be different from the surface PEGylation control between low-pressure and atmospheric-pressure plasma treatments.

To achieve the desired grafting coverage of PEGMA layers on the PVDF membrane surface, the plasma treatment time for the resulting membranes was adjusted in the range of 120 s under the defined control of PEGMA monomer coating of about $1 \text{ mg}/\text{cm}^2$ for each plasma-induced surface PEGylation. PVDF-g-PEGMA membrane prepared using ozone pretreatment and thermally induced radical copolymerization was also studied for comparison. The modification process was similar to that previously reported.⁹ In this work, different approaches of surface PEGylation of PVDF membranes are summarized in Table 1. The surface grafting yield (mg/cm^2) of the modified PVDF membrane is defined as the weight difference between the modified PVDF membrane and the virgin PVDF membrane divided by the surface area of the virgin PVDF membrane. It was found that a highly efficient grafting copolymerization was obtained using plasma-induced surface PEGylation. The presence of grafted PEGMA polymer on the PVDF membrane surface is characterized by FT-IR measurement, for which the typical spectrum was shown in Figure 2. The grafted PEGMA can be ascertained from the ester carbonyl groups attributable to the band for the $\text{O}-\text{C}=\text{O}$ stretch at 1727 cm^{-1} , which obviously appears on the PEGylated PVDF membranes. The ratio of the intensity of the adsorption band for $\text{O}-\text{C}=\text{O}$ at 1727 cm^{-1} to that of the adsorption band for $\text{C}-\text{F}$ at 1400 cm^{-1} ($[\text{O}-\text{C}=\text{O}]/[\text{C}-\text{F}]$ ratio) reflects the relative graft amount of PEGMA on the PVDF membrane surface. It was found that both the intensity of the $\text{O}-\text{C}=\text{O}$ adsorption at 1727 cm^{-1} and the $[\text{O}-\text{C}=\text{O}]/[\text{C}-\text{F}]$ ratio increased obviously as the plasma treatment time was increased from 5 to 120 s. The result indicates that the growth

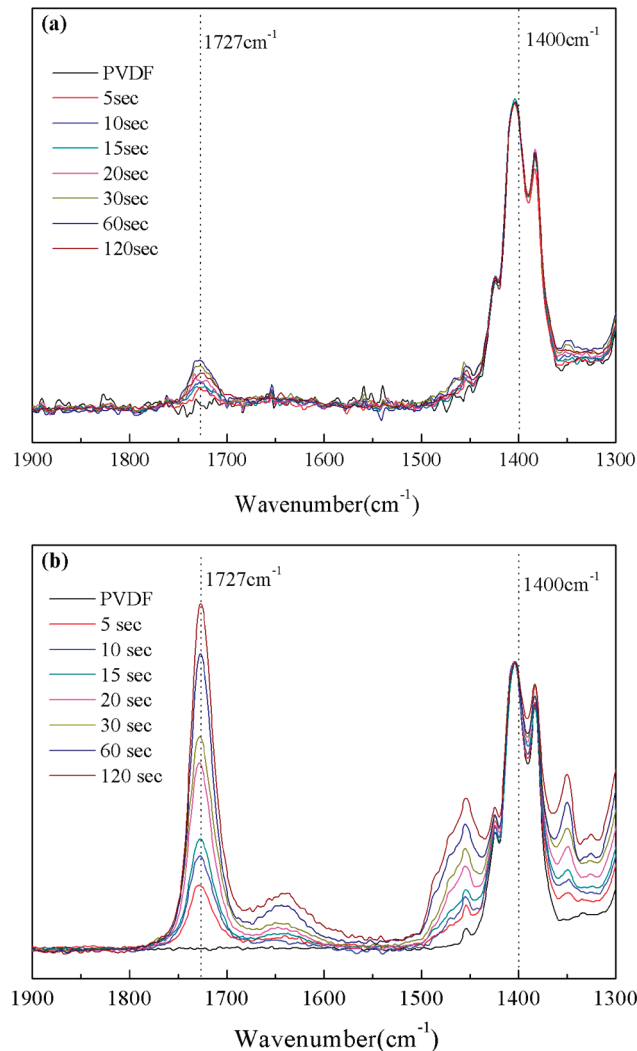


Figure 2. FT-IR spectra of PVDF membranes grafted with PEGMA polymer via (a) low-pressure plasma treatment; (b) atmospheric plasma treatment.

of the grafted PEGMA polymer is dependent on the grafting time during low-pressure and atmospheric plasma treatment. It was also found that the intensity of the adsorption band at 1727 cm^{-1} for atmospheric plasma treatment is higher than that for low-pressure plasma treatment, which indicated the formation of a PEGMA-grafted polymer on the top layer of the PVDF membrane via atmospheric plasma-induced surface PEGylation.

As shown in Figure 3, the grafting yield of grafted PEGMA layers on the surface of PVDF membranes increased as the

plasma treatment time increased from 5 to 120 s. It provides a significant practical insight that plasma-induced surface PEGylation can be performed at an efficient grafting time, as listed in Table 1, compared to thermally induced surface PEGylation. The reduced values of the water contact angle in Figure 3 indicate that the surface hydrophilicity of PVDF-g-PEGMA membranes increases with increasing surface coverage of hydrophilic grafted PEGMA polymer on the hydrophobic PVDF membranes. The water contact angle of the PVDF-g-PEGMA membrane surface was as low as about 20°, indicating an obvious increase in hydrophilicity compared to the virgin PVDF membrane surface. It was also found that there appeared to be an almost unchanged value of the water contact angle as the grafting yield reached

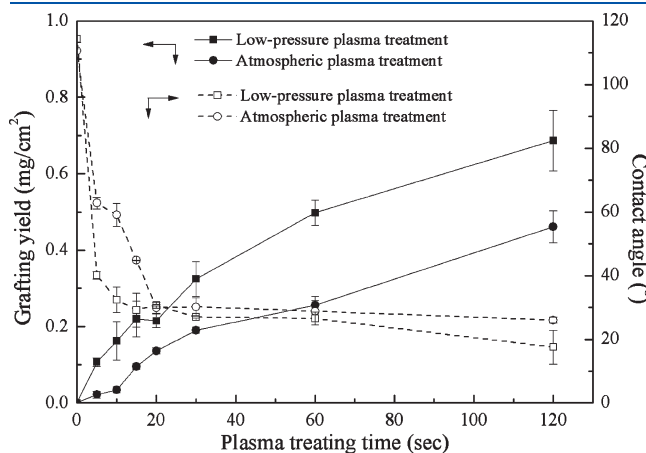


Figure 3. Changes in the surface grafting yield and water contact angle of PVDF-g-PEGMA membranes as a function of plasma treatment time during low-pressure and atmospheric plasma treatment, respectively.

>0.2 mg/cm². This indicates that grafted PEGMA polymer on the PVDF membrane surface approaches its respective saturated coverage with steady water contact angle.

Surface Morphology of the PEGylated PVDF Membranes. Surface morphology of the PEGylated membranes is associated with the surface coverage and chain conformation of grafted PEGMA polymer on the PVDF membrane, which was observed by SEM and bio-AFM. In Figure 4, the surface coverage and skin layer of the PVDF-g-PEGMA membrane revealed an obvious change as the plasma treatment time was increased from 5 to 60 s. After the surface plasma treatment of 60 s, it could be observed in a dry state from the SEM surface images in Figure 4d and k that the porous structure on the PVDF membrane surface was almost covered with grafted PEGMA polymer. Grafting amount of PEGMA obtained from the measurements of the [O—C=O]/[C—F] ratio characterized by FT-IR showed an increased value as the plasma treatment time increased, which was consistent with the results of a change in morphology on the PVDF-g-PEGMA membrane surface from SEM. According to the surface images in Figure 4b–d using low-pressure plasma treatment and that in Figure 4i–k using atmospheric plasma treatment, it clearly indicated that the decrease of water contact angle on the membrane surface was due to the increase in surface coverage of grafted PEGMA polymer. As shown in the cross-sectional images of Figure 4l–n, a clear skin layer formation of grafted PEGMA polymer on the PVDF membrane surface was obtained using atmospheric plasma-induced surface PEGylation. The thickness of the grafted PEGMA layer on the PVDF-g-PEGMA#2 membrane can be controlled at about 1 μm within a short plasma treatment time of 60 s. As compared with low-pressure plasma treatment, the relatively high grafting yield shown in Figure 3 but no obvious skin layer formation observed in Figure 4f–h suggested that grafted PEGMA polymer could

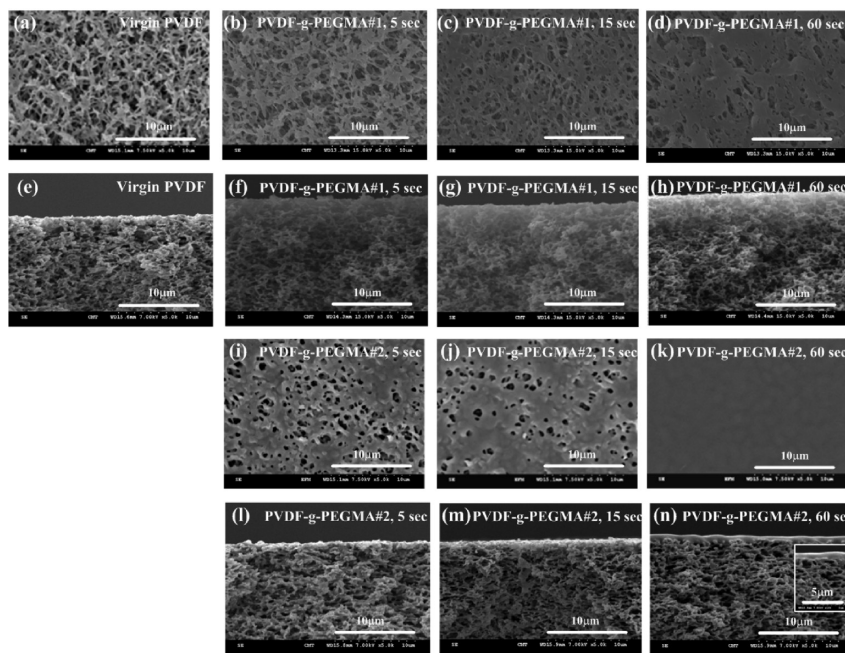


Figure 4. SEM images of surface morphology and cross-sectional structure of the PVDF-g-PEGMA membranes: surface images and cross-sectional images in (a) and (e) of virgin PVDF membrane; the sequence in b–d and f–h of PVDF-g-PEGMA#1 membranes using low-pressure plasma treatment with the plasma treatment times of 5, 15, and 60 s; the sequence in i–k and l–n of PVDF-g-PEGMA#2 membranes using atmospheric plasma treatment with the plasma treatment times of 5, 15, and 60 s. All images with magnification of 5000×.

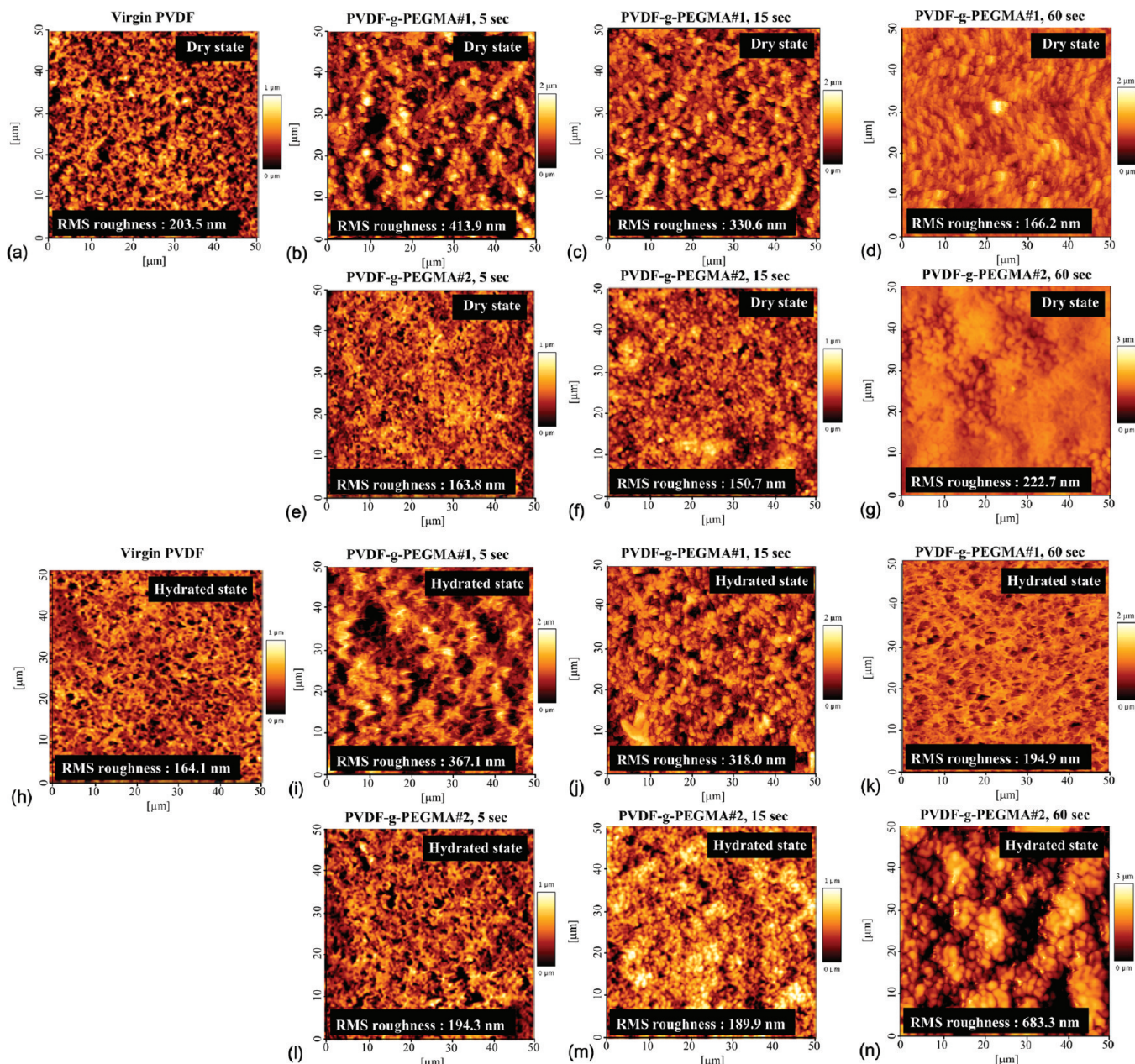


Figure 5. Tapping-mode bio-AFM images of surface morphology and rms roughness of the PVDF-g-PEGMA membranes: surface images in dry state of (a) virgin PVDF membrane, and the sequence in (b–d) of PVDF-g-PEGMA#1 membranes using low-pressure plasma treatment and (e–g) of PVDF-g-PEGMA#2 membranes using atmospheric plasma treatment with the plasma treatment times of 5, 15, and 60 s, respectively; surface images in hydrated state of (h) virgin PVDF membrane, and the sequence in (i–k) of PVDF-g-PEGMA#1 membranes using low-pressure plasma treatment and (l–n) of PVDF-g-PEGMA#2 membranes using atmospheric plasma treatment with the plasma treatment times of 5, 15, and 60 s, respectively. The dimensions of the scan images are 50.0 $\mu\text{m} \times 50.0 \mu\text{m}$.

actually exist on the surface deep inside the pores of PVDF-g-PEGMA#1 membrane.

The increase in surface grafting coverage associated with the increase in the thickness of the PEGMA layer resulted in the nearly constant water contact angle, indicating that grafted PEGMA polymer on the PVDF membrane surface approaches its respective saturated coverage with steady water contact angle. The results confirmed previous statements that the value of the water contact angle is sensitive to the surface area of hydrophilic coverage rather than the surface layer of hydrophilic thickness.^{9,13} However, it should be noted that the change in water contact

angle is usually not a good indication of the degree of hydration on the highly hydrophilic surface coverage. Figure 5 showed the bio-AFM images of the conformational structure of grafted PEGMA polymer on the PVDF membrane surfaces that were observed in the dry state under atmospheric environment and in the hydrated state under an aqueous solution at 37 °C. It was interesting to observe that these PEGylated membrane surfaces display different images of Figure 5b–g in the dry state and that of Figure 5i–n in the hydrated state, while the virgin PVDF images in Figure 5a and h keep the same surface morphology. As the high surface coverage of grafted PEGMA polymer was

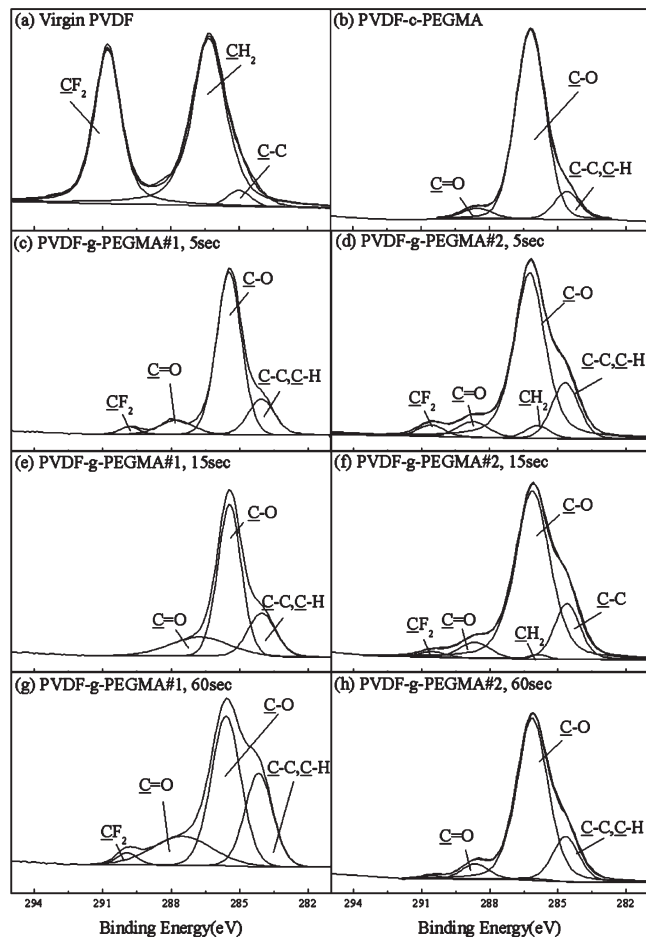


Figure 6. C_{1s} core-level spectra of the (a) virgin PVDF membrane, (b) PVDF-c-PEGMA, PVDF-g-PEGMA#1 from (c) 5 s, (e) 15 s, and (g) 60 s of low-pressure plasma treatment, and PVDF-g-PEGMA#2 from (d) 5 s, (f) 15 s, and (h) 60 s of atmospheric plasma treatment.

obtained from both plasma treatments at 60 s, the pores on the PVDF membrane surface were almost fully covered in the dry state as shown in Figure 5d,g. From atmospheric plasma-induced surface PEGylation, an obvious change in the surface roughness of PVDF-g-PEGMA#2 membrane from dry state (~ 220 nm) to hydrated state (~ 680 nm) indicated that surface grafted PEGMA layers could keep their well-extended conformation in an aqueous liquid phase due to the good hydration with water molecules. However, from low-pressure plasma-induced surface PEGylation, less change in the surface roughness of the PVDF-g-PEGMA#1 membrane from dry state (~ 160 nm) to hydrated state (~ 195 nm) indicated that surface grafted PEGMA layers could retain their chain conformation with the confined hydration. The results indicate that the conformational structures of grafted PEGMA polymer on PVDF membrane surface are associated with the different preparation approach using low-pressure and atmospheric plasma-induced surface PEGylation. The AFM results suggest that atmospheric plasma-induced surface PEGylation is a well-controlled process to prepare the hydrophilic PVDF membrane surface with a uniform distribution of highly hydrated PEGMA layers.

Correlation of Grafting Structure and Hydration Capability of the PEGylated PVDF Membranes. In general, the evaluation of protein adsorption on the hydrated membrane

surfaces should consider not only the surface hydrophilicity and hydration capability but also the surface grafting structure of the hydrophilic layer on the prepared membranes.^{25–28} In this study, grafting structures of the PEGMA layer on the PVDF membrane surface were identified by XPS analysis. Figure 6 shows the typical XPS spectrum of the virgin PVDF membrane and the PEGylated PVDF membranes. The C_{1s} core-level spectrum of the membranes was curve-fitted with peak components for the $[C-C]$, $[C-H]$, $[C-O]$, and $[C=O]$ species, at the binding energies of about 284.6, 286.5, and 288.8 eV, respectively. The characterization results of coated or grafted PEGMA layer on the PVDF membranes are summarized in Table 2. By XPS analysis of the elemental compositions of the PVDF membrane coated with PEGMA macromonomer (PVDF-c-PEGMA), the peak component area ratio of $[C-C]/[C-H]/[C-O]/[C=O]$ for the chemical structure of PEGMA macromonomer used in this study is about 2.86:19.40:1, which is in good agreement with the theoretical ratio of 3:20:1 for the chemical structure of PEGMA with an average number of ethylene glycol units of about 10. From composition analysis summarized in Table 2, the $[C-O]/[C=O]$ ratio of the PVDF-g-PEGMA#1 decreased to ~ 3.9 and that of PVDF-g-PEGMA#2 decreased to ~ 12.9 as the plasma treatment time increased to 60 s, which indicates the typical plasma treatment at low pressure resulting in high chemical degradation of the ethylene glycol structure. Interestingly, it was found that the $[C-C]/[C=O]$ ratio remained almost unchanged from atmospheric plasma-induced surface PEGylation, which is similar to the theoretical value of 3.0, as the increase of plasma treatment time, indicating that a limited cross-linking reaction occurs between PEGMA chains or between PEGMA chains and the PVDF membrane surface. However, the $[C-C]/[C-H]/[C=O]$ ratio of the PVDF-g-PEGMA#1 using low-pressure plasma-induced surface PEGylation is deviated more than 3.0, which indicates that the cross-linking reaction occurs between PEGMA chains or between PEGMA chains and the PVDF membrane surface. As shown in Figure 1, low-pressure plasma-induced surface PEGylation resulted in the formation of a network-like PEGMA layer on the PVDF-g-PEGMA#1 membrane surface with high chemical degradation of the ethylene glycol structure. However, the grafting structure of brush-like PEGMA layer on the surface of the PVDF-g-PEGMA#2 membrane with low chemical degradation of the ethylene glycol structure was obtained using atmospheric plasma-induced surface PEGylation. In this study, the PEGylated layer on PVDF is brush-like with a long PEG side chain in the initial stage of plasma-induced grafting. However, during subsequent plasma irradiation, although the grafted layer is in growth, bond scission in the grafted polymer and the cross-linking reaction may occur, resulting in the formation of a network-like PEGylated layer on the substrates. In general, bond scission in the grafted layer requires the ions, electrons, and argon metastables in the plasma gas to diffuse through a coated monomer layer (few micrometers thick) and then react with the grafted polymer. Since the diffusivity of the plasma species is proportional to the reciprocal of pressure, the bond scission and cross-linking reaction should be much less in the PEGylated layer obtained by atmospheric-pressure plasma treatment than by low-pressure plasma treatments (operated at 0.5 Torr in this study). Thus, the PEGylated layer is relatively brush-like by atmospheric-pressure plasma treatment, while it is more network-like by low-pressure plasma treatments.

Table 2. Surface Characterization of PEGMA Composition on the PVDF Membranes

samples	plasma treating time	compositions of grafting PEGMA layer (mol %)				
		[C—C, C—H]	[C—O]	[C=O]	[C—C, C—H]/[C=O]	[C—O]/[C=O]
PEGMA ^a	-	12.50	83.34	4.16	3.00	20.00
PVDF-c-PEGMA ^b	-	12.30	83.40	4.30	2.86	19.40
PVDF-g-PEGMA#1 ^c	5 s	19.59	77.02	3.39	5.77	22.71
	15 s	25.06	67.69	7.25	3.46	9.34
	60 s	38.44	49.03	12.53	3.07	3.91
PVDF-g-PEGMA#2 ^d	5 s	6.13	71.87	18.14	2.96	11.73
	15 s	5.71	75.14	17.40	3.04	13.15
	60 s	5.86	75.57	17.80	3.04	12.90

^aTheoretical compositions of PEGMA macromonomer. ^bMembranes coated with 1.0 mg/cm² of PEGMA monomer from 10 wt % solution.

^cMembranes prepared by plasma-induced surface PEGylation using low-pressure plasma treatment. ^dMembranes prepared by plasma-induced surface PEGylation using atmospheric plasma treatment.

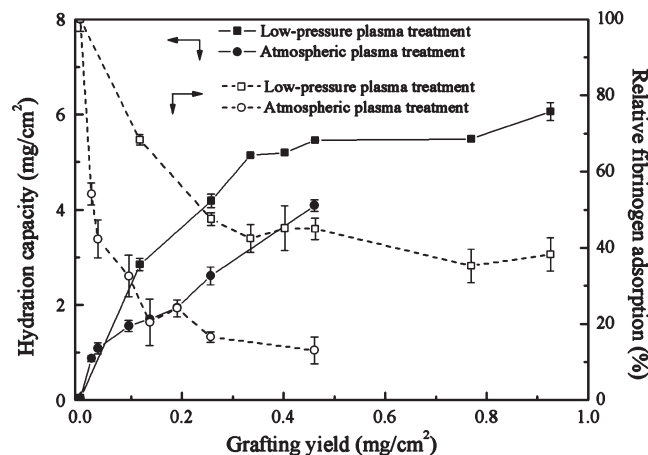


Figure 7. Changes in the hydration capacity and relative protein adsorption of PVDF-g-PEGMA membranes as a function of PEGMA grafting yield using low-pressure and atmospheric plasma treatments, respectively.

The formation of the bounded water layer on a highly hydrated surface was considered as a crucial issue to repel plasma proteins and made the antithrombogenic surface generated.^{4,26} In general, the surface structure of grafted hydrophilic polymer, such as chain length and chain conformation, is associated with the capacity of water molecules on the hydrated surface.²⁸ In this study, hydration capacity (mg/cm²) of the prepared membrane is defined as the difference in wet weight between the PEGMA grafted PVDF membrane and the virgin PVDF membrane divided by the total surface area of the virgin PVDF membrane. Figure 7 shows the dependence of hydration capacity and relative fibrinogen adsorption of the modified PVDF membranes on the surface grafting yield of PEGylated layer that can be controlled by the plasma treatment time. The measured quantity of hydration capacity may undergo the following three types of contribution: (1) trapping water molecules in the porous structure of the PVDF membrane, (2) binding water molecules around the ethylene glycol structure of the PEGMA brushes, and (3) captured water molecules in the confined space between cross-linked PEGMA chains. The result in Figure 7 indicated that no hydration of the virgin PVDF membrane was obtained, which is attributed to the lack of trapping water molecules in the porous

structures. In general, the increase in grafting yield associated with the increase in the thickness of the PEGMA layer resulted in the increased quantity of hydration capacity, which is dependent on the contribution of binding and captured water molecules. The results showed that the hydration capacity of PVDF-g-PEGMA#1 is higher than that of PVDF-g-PEGMA#2 at the same PEGMA grafting yield of about 0.45 mg/cm², which is due to the fact that the confined space for captured water molecules in the grafting structure of network-like PEGMA layers is more than that of brush-like PEGMA layers. It should be noted that the increase of hydration capacity on the PVDF-g-PEGMA#2 membranes was observed. This is due to the increase in surface grafting associated with the increase in both coverage and thickness of brush-like PEGMA layers resulting in the increasing capacity of the hydration for the PEGMA chain grafted on the membrane surface.

In Figure 7, it was found that reduction in nonspecific fibrinogen adsorption exhibited a positive correlation with the variation of the hydration capacity of PVDF-g-PEGMA membranes. It can be seen that the relative protein adsorption on PVDF-g-PEGMA#2 is effectively reduced to 15% of that on virgin PVDF as the hydration capacity increased to 4 mg/cm², indicating that the grafting structure of the brush-like PEGMA layer can highly resist nonspecific protein adsorption. However, the relative protein adsorption on PVDF-g-PEGMA#1 is only reduced to the limitation at 40% of that on virgin PVDF, even as the hydration capacity increased to 6 mg/cm². The results may be related to the types of water molecules in the hydrated layer and the grafting structure of the PEGMA layer on the PVDF membrane surface. As shown in Figure 6, the grafting structure of network-like PEGMA layers on PVDF-g-PEGMA#1 provides greater hydration capacity of captured water molecules than that of binding water molecules, as indicated by the degradation of ethylene glycol structure and the cross-linking of PEGMA chains. In general, the binding water molecules around the PEGMA structure decreased with the decrease in the repeated units of ethylene glycol. On the basis of the current studies of the general antifouling mechanism, it is acceptable to consider that the binding water molecules around the pendent groups of the antifouling chains play a key role in providing resistance to protein adsorption.^{26,27} Thus, the observed results indicate that the brush-like PEGylated layer present higher hydration capability with binding water molecules than the network-like PEGylated layer. These results also suggest that the general

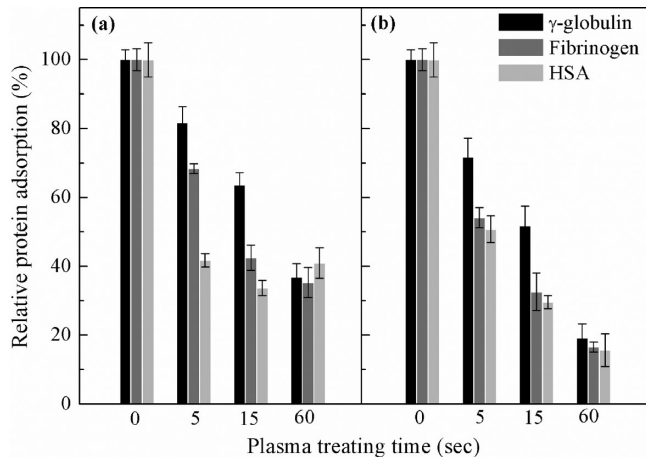


Figure 8. Relative human plasma protein (γ -globulin, fibrinogen, and HSA) adsorption from platelet poor plasma solution on PVDF-g-PEGMA membranes with 0, 5, 15, and 60 s of (a) low-pressure plasma treatment and (b) atmospheric plasma treatment, respectively. All data was determined from ELISA with the virgin PVDF membrane as a reference, where the amount of each protein adsorbed on PVDF was normalized to unity. Data are expressed as the means \pm SD of three independent measurements.

evaluation of protein adsorption on the hydrated membrane surfaces should be considered not only the surface hydrophilicity and hydration capacity, but also the grafting structure of the PEGylated surface.

Surface Hemocompatibility of the PEGylated PVDF Membranes. Horbett et al. showed that the adhesion and activation of platelets from the bloodstream might be correlated with the adsorption of plasma proteins on surfaces.^{29,30} In general, it was believed that the ability of a membrane surface to resist plasma protein adsorption, especially for fibrinogen, is a prerequisite for a membrane surface to resist blood platelet adhesion.⁶ Therefore, the adsorption of plasma proteins to a membrane usually provides a good indication of the membrane performance of the hemocompatibility. An incubated solution containing human plasma proteins from 100% PPP solution was used in this study to estimate the hemocompatibility of the prepared membranes of PVDF-g-PEGMA at human body temperature (37 °C). The relative protein adsorption of γ -globulin, fibrinogen, and HSA from PPP solution on the membranes was evaluated using ELISA test with monoclonal antibodies. ELISA results for the relative plasma protein adsorption are reported in Figure 8. We observed significant decreases in the adsorption of plasma proteins on the PVDF-g-PEGMA membranes as compared to pristine PVDF membrane at 37 °C. Similar to reductions in the aforementioned single protein adsorption of fibrinogen, brush-like PEGylated layers on the PVDF-g-PEGMA#2 membrane present higher resistance of plasma protein adsorption than network-like PEGylated layers on the PVDF-g-PEGMA#1 membrane. In Figure 8b, the amount of fibrinogen adsorbed on the hydrophobic surface of the pristine PVDF membrane from plasma solution is 80% higher than that on the PVDF-g-PEGMA#2 membrane with a surface grafting coverage of 0.25 mg/cm² at an atmospheric plasma treatment time of 60 s. As in the aforementioned results in Figure 4, it was noted that the relative protein adsorption from human plasma was effectively reduced with increasing surface grafting coverage and hydration capacity of the PEGMA chain grafted on the membrane surface. However, the

results also showed that the adsorption of plasma proteins on the membranes from human plasma still performs the partial irreversible biofouling for the highly PEGMA-grafted membranes. It is generally accepted that the increase of hydrophilic PEGylated moieties on a hydrophobic surface can effectively reduce protein adsorption due to the decrease in hydrophobic interactions between the protein and the hydrophobic patches. Two possible phenomena may be related to the reduction in plasma protein adsorption on the prepared PVDF-g-PEGMA membranes. One is the surface grafting of PEGMA chains which inhibits plasma protein adsorption. The other is the blocking of inside pores by the grafted PEGMA chains. After surface PEGylation using plasma treatment, there is still 20–40% of plasma protein adsorption as compared to the untreated PVDF membrane. This might be due to the nearby hydrophobic patches of cross-linked PEGMA chains or the partial hydrophobic surface of uncovered PEGMA chains on the top surface or the inside pores of prepared PVDF-g-PEGMA membranes. The results demonstrated that the chemically inert surface of PVDF could be successfully grafted with PEGMA chains, and the plasma protein adsorption on the membrane surface could be greatly reduced because of the surface PEGylation.

The human platelet adhesion test has already become a recognized technique to estimate the hemocompatibility of a prepared membrane surface.^{4,9,13} Thus, our work also employed this test to evaluate the hemocompatibility of the PVDF-g-PEGMA membrane surface. The morphology of adhering platelets on the membranes was obtained from SEM images at a 1000 \times magnification from five different places on the same membranes. In the SEM images of Figure 9a–g, the surface images were shown of the virgin PVDF membrane and PVDF-g-PEGMA membranes without contact with human plasma solution. Figure 9h–n showed SEM images of platelets that adhered to the membrane surfaces by the contact of the prepared membranes with the recalcified PRP solution for 60 min at 37 °C in vitro. It is clearly observed that the platelets have spread on the virgin PVDF membrane, which indicates the activation of the platelets as shown in Figure 9h. However, the SEM images in Figure 9i–n showed that the platelet adhesion was remarkably suppressed on PEGMA-grafted PVDF membranes as compared with the virgin PVDF membrane. This result revealed that there was no observed platelet adhesion to brush-like PEGylated layers on the PVDF-g-PEGMA#2 membrane surface, even with a low surface coverage of grafted PEGMA polymer. However, single platelet adhesion to network-like PEGylated layer was observed on PVDF-g-PEGMA#1 membrane surfaces with a low surface coverage of grafted PEGMA polymer. The excellent performance of all prepared PVDF-g-PEGMA#2 membranes in no obvious adhesion and activation of blood platelets is due to their ability to highly resist nonspecific protein adsorption from blood plasma. These results strongly suggest that the well-hydrated surface of brush-like PEGMA-grafted PVDF membranes prepared by atmospheric plasma-induced PEGylation could efficiently reduce protein adsorption, suppress platelet adhesion/activation, and increase its hemocompatibility.

It is generally acknowledged that nonspecifically adsorbed plasma proteins interact in a series of reactions leading to plasma clotting.^{4,5,29–32} Among plasma proteins, fibrinogen plays a leading role in mediating surface-induced activation as polymeric membranes contact human blood plasma under static conditions.⁴ The measurement of plasma clotting has already become a recognized test to estimate the blood compatibility of a prepared

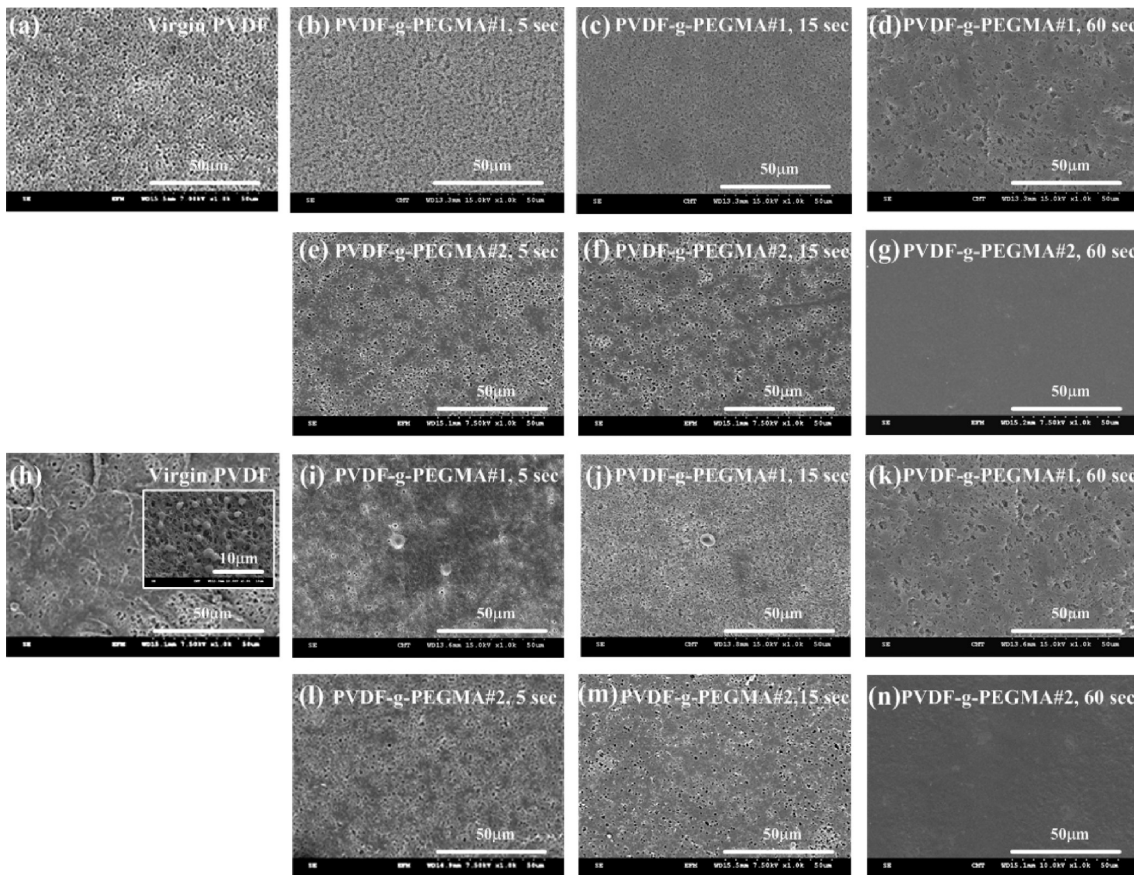


Figure 9. SEM images of platelets adhered onto the surface of the modified PVDF membranes with grafted PEGMA: (a and h) of virgin PVDF membrane; the sequence in (b–d), (e–g), (i–k), and (l–n) of PVDF-g-PEGMA membranes with the plasma treatment times of 5, 15, and 60 s, respectively. The prepared membranes of (a–g) without contact to the PRP solution, and (h–n) with contact to the recalcified PRP solution, respectively. All images with magnification of 1000 \times .

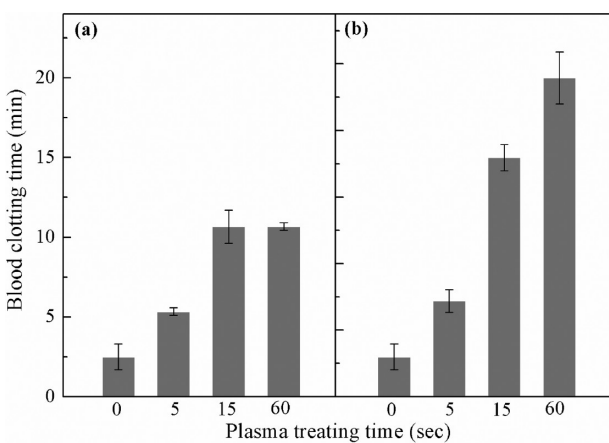


Figure 10. Plasma-clotting time of recalcified platelet-poor plasma in the presence of PVDF-g-PEGMA membranes with 0, 5, 15, and 60 s of (a) low-pressure plasma treatment and (b) atmospheric plasma treatment, respectively. Clotting time for blank PS wells was about 10 min at 37 °C. Each clotting time is an average value of six samples.

membrane.⁵ The prepared membranes of PVDF-g-PEGMA#1 and PVDF-g-PEGMA#2 were directly incubated with human plasma to inspect the effects of direct-contact activation on polymer-induced plasma clotting as evaluated by their recalcified

plasma clotting times. 0.5 mL of recalcified human PPP solution was added to each membrane sample with 0.4 cm² in a PS 24-well plate at physiological temperature of 37 °C. In general, the plasma clotting for the recalcified plasma solutions in blank PS wells was determined to have an upper limit of plasma-clotting time of about 10 min at 37 °C for the protocol used. In Figure 10, when the recalcified PPP solution was added to the hydrophobic PVDF membrane, the clotting time decreased to ~2.5 min. The result indicates that the hydrophobic surface is a highly activating polymer which activates plasma clotting through the intrinsic coagulation pathway. The average clotting time increased with the increase of plasma treatment time, which is attributed to the surface coverage of hydrated PEGMA layers on the PVDF membrane surface. In Figure 10a, almost no change in plasma clotting time in the absence or presence of PVDF-g-PEGMA#1 membranes was observed as the PEGMA grafting yield increased above 0.2 mg/cm². The results indicate that network-like PE-Gylated layers on PVDF-g-PEGMA#1 membrane surface do not activate plasma clotting through the intrinsic coagulation pathway. In Figure 10b, it is interesting to observe that, when the recalcified PPP solution was added to PVDF-g-PEGMA#2 membrane, the average clotting time increased to 20 min as the PEGMA grafting yield reached above 0.2 mg/cm². The clotting time of PPP was prolonged and increased with the grafting yield of the grafted PEGMA polymer, indicating anticoagulant activity of brush-like PE-Gylated layers on

PVDF-g-PEGMA#2 membrane surfaces. Thus, the general concept for preparing antithrombogenic membranes from chemically inert PVDF materials could be performed in the ease of plasma-induced surface PEGylation, but it should concern the issue of surface grafting coverage and structures of PEGylated nonfouling nature in human blood.

■ CONCLUSIONS

In this work, hemocompatible PEGylated PVDF membranes with controllable grafting coverage and structures were obtained via plasma-induced surface PEGylation. Two surface grafting structures of network-like and brush-like PEGylated layers on PVDF membranes were achieved. Herein, for the first time, the present study has shown that brush-like PEGMA layer on the PVDF membrane surface using the atmospheric plasma technique is a promising approach to the preparation of membranes with low chemical degradation and limited cross-linking of ethylene glycol structure, which is different from the general observation using low-pressure plasma treatment. We found that the PVDF membrane grafted with a brush-like PEGylated layer presents a higher hydration capability of binding water molecules and lower protein adsorption of human fibrinogen than that with network-like PEGylated layers. The blood compatibility of the PEGylated PVDF membranes in human blood was characterized with respect to plasma-protein adsorption and blood-platelet adhesion from human plasma solution and to recalcified plasma clotting time at the physiological temperature. The results showed that PEGylated PVDF membranes exhibited a nonfouling character for plasma-protein and blood-platelet resistance that depended on the surface grafting coverage and structures of the PEGylated layer on PVDF membranes. Importantly, the membrane grafted with a brush-like PEGylated layer presented excellent anticoagulant activity in human blood, which was attributed to the formation of a strong interfacial hydration layer due to the binding of water molecules around un-cross-linked PEG chains. This study suggests that controlling grafting anti-fouling structures from plasma-induced surface PEGylation gives the hemocompatible PEGylated PVDF membranes great potential in the ideal design of antithrombogenic membranes for use in human blood.

■ AUTHOR INFORMATION

Corresponding Author

* E-mail: ychang@cycu.edu.tw; tcwei@cycu.edu.tw.

■ ACKNOWLEDGMENT

The authors wish to express their sincere gratitude to the Center-of-Excellence (COE) Program on Membrane Technology from the Ministry of Education (MOE), R.O.C., and the National Science Council (NSC 99-2628-E-033-001 and NSC 99-2221-E-033-001-MY2) for their financial support.

■ REFERENCES

- (1) Hoffman, A. S. *Advances in Chemistry Series*; American Chemical Society: Washington, DC, 1982; p 3.
- (2) Ratner, B. D.; Hoffman, A. D.; Schoen, F. D.; Lemons, J. E. *Biomaterials Science, an Introduction to Materials in Medicine*, 2nd ed.; Elsevier: Amsterdam, 2004.
- (3) Ratner, B. D. *Biomaterials* **2007**, *28*, 5144–5147.

- (4) Zhang, Z.; Zhang, M.; Chen, S.; Horbett, T. A.; Ratner, B. D.; Jiang, S. *Biomaterials* **2008**, *29*, 4285–4291.
- (5) Chang, Y.; Shu, S. H.; Chu, C. W.; Shih, Y. J.; Ruaan, R. C.; Chen, W. Y. *Langmuir* **2010**, *26*, 3522–3530.
- (6) Tsai, W. B.; Grunkemeier, J. M.; Horbett, T. A. *J. Biomed. Mater. Res.* **1999**, *44*, 130–139.
- (7) Ostuni, E.; Chapman, R. G.; Holmlin, R. E.; Takayama, S.; Whitesides, G. M. *Langmuir* **2001**, *17*, 5605–5620.
- (8) Lin, D. J.; Lin, D. T.; Young, T. H.; Huang, F. M.; Chen, C. C.; Cheng, L. P. *J. Membr. Sci.* **2004**, *245*, 137–146.
- (9) Chang, Y.; Shih, Y. J.; Ruaan, R. C.; Higuchi, A.; Chen, W. Y.; Lai, J. Y. *J. Membr. Sci.* **2008**, *309*, 165–174.
- (10) Rana, D.; Matsuura, T. *Chem. Rev.* **2010**, *110*, 2448–2471.
- (11) Balakrishnan, B.; Kumar, D. S.; Yoshida, Y.; Jayakrishnan, A. *Biomaterials* **2005**, *26*, 3495–3502.
- (12) Wang, P.; Tan, K. L.; Kang, E. T.; Neoh, K. G. *J. Mater. Chem.* **2001**, *11*, 783–789.
- (13) Chang, Y.; Cheng, T. Y.; Shih, Y. J.; Lee, K. R.; Lai, J. Y. *J. Membr. Sci.* **2008**, *323*, 77–84.
- (14) Kang, E. T.; Zhang, Y. *Adv. Mater.* **2000**, *12*, 1481–1494.
- (15) Dargaville, T. R.; George, G. A.; Hill, D. J. T.; Whittaker, A. K. *Prog. Polym. Sci.* **2003**, *28*, 1355–1376.
- (16) Wang, P.; Tan, K. L.; Kang, E. T.; Neoh, K. G. *J. Membr. Sci.* **2002**, *195*, 103–114.
- (17) Chen, Y.; Ying, L.; Yu, W.; Kang, E. T.; Neoh, K. G. *Macromolecules* **2003**, *36*, 9451–9457.
- (18) Zhai, G.; Kang, E. T.; Neoh, K. G. *Macromolecules* **2004**, *37*, 7240–7249.
- (19) Chen, Y.; Deng, Q.; Xiao, J.; Nie, H.; Wu, L.; Zhou, W.; Huang, B. *Polymer* **2007**, *48*, 7604–7613.
- (20) Chiang, Y. C.; Chang, Y.; Higuchi, A.; Chen, W. Y.; Ruaan, R. C. *J. Membr. Sci.* **2009**, *339*, 151–159.
- (21) Chang, Y.; Ko, C. Y.; Shih, Y. J.; Que'mener, D.; Deratani, A.; Wei, T. C.; Wang, D. M.; Lai, J. Y. *J. Membr. Sci.* **2009**, *345*, 160–169.
- (22) Zhao, Y. H.; Zhu, B. K.; Kong, L.; Xu, Y. Y. *Langmuir* **2007**, *23*, 5779–5786.
- (23) Zhao, Y. H.; Qian, Y. L.; Pang, D. X.; Zhu, B. K.; Xu, Y. Y. *J. Membr. Sci.* **2007**, *304*, 138–147.
- (24) Chen, Y. W.; Liu, D. M.; Deng, Q. L.; He, X. F. *J. Polym. Sci., Part A: Polym. Chem.* **2006**, *44*, 3434–3443.
- (25) Zheng, J.; Li, L.; Chen, S.; Jiang, S. *Langmuir* **2004**, *20*, 8931–8938.
- (26) He, Y.; Chang, Y.; Hower, J.; Zheng, J.; Chen, S.; Jiang, S. *Phys. Chem. Chem. Phys.* **2008**, *10*, 5539–5544.
- (27) He, Y.; Hower, J.; Chen, S.; Bernards, M. T.; Chang, Y.; Jiang, S. *Langmuir* **2008**, *24*, 10358–10364.
- (28) Chang, Y.; Chu, W. L.; Chen, W. Y.; Zheng, J.; Liu, L. Y.; Ruaan, R. C.; Higuchi, A. *J. Biomed. Mater. Res.* **2010**, *93*, 400–408.
- (29) Shen, M. C.; Wagner, M. S.; Castner, D. G.; Ratner, B. D.; Horbett, T. A. *Langmuir* **2003**, *19*, 1692–1699.
- (30) Kwak, D.; Wu, Y. G.; Horbett, T. A. *J. Biomed. Mater. Res., Part A* **2005**, *74A*, 69–83.
- (31) Grunkemeier, J. M.; Tsai, W. B.; Horbett, T. A. *J. Biomed. Mater. Res.* **1998**, *41*, 657–670.
- (32) Cao, L.; Chang, M.; Lee, C. Y.; Castner, D. G.; Sukavaneshvar, S.; Ratner, B. D. *J. Biomed. Mater. Res., Part A* **2007**, *81A*, 827–837.